Comparison of PSMA PET/CT with fluoride PET/CT for detection of bone metastatic disease in prostate cancer

Naresh Kumar Regula (naresh.regula@surgsci.uu.se)
Uppsala University Hospital: Akademiska sjukhuset https://orcid.org/0000-0002-7499-4787
Vasileios Kostaras
Uppsala University Hospital: Akademiska sjukhuset
Silvia Johansson
Uppsala University Hospital: Akademiska sjukhuset
Carlos Trampal
Uppsala University Hospital: Akademiska sjukhuset
Elin Lindström
Uppsala University Hospital: Akademiska sjukhuset
Mark Lubberink
Uppsala University Hospital: Akademiska sjukhuset
Victor Iyer
Uppsala University Hospital: Akademiska sjukhuset
Irina Velikyan
Uppsala University Hospital: Akademiska sjukhuset
Jens Sörensen
Uppsala University Hospital: Akademiska sjukhuset

Research Article

Keywords: PSMA, fluoride, prostate cancer, PET/CT

Posted Date: September 1st, 2021

DOI: https://doi.org/10.21203/rs.3.rs-776117/v1

Abstract

^{18}F-NaF positron emission tomography/computed tomography (fluoride PET/CT) is considered the most sensitive technique to detect bone metastasis in prostate cancer (PCa). ^{68}Ga-PSMA-11 (PSMA) PET/CT is increasingly used for staging of PCa. This study primarily aimed to compare the diagnostic performance of fluoride PET/CT and PSMA PET/CT in identifying bone metastasis followed by a comparison of PSMA PET/CT with contrast-enhanced CT (CE-CT) in identifying soft tissue lesions as a secondary objective.

Methods: Twenty-eight PCa patients with high suspicion of disseminated disease following curative treatment were prospectively evaluated. PET/CT examinations using fluoride and PSMA were performed. All suspicious bone lesions were counted, and the tracer uptake was measured as standardized uptake values (SUV) for both tracers. In patients with multiple findings, ten bone lesions with highest SUV_{max} were selected from which identical lesions from both scans were considered for direct comparison of SUV_{max}. PSA at scan was correlated with findings of both scans.

Results: Both scans were negative for bone lesions in 7 patients (25%). Of 699 lesions consistent with skeletal metastasis in 21 patients on fluoride PET/CT, PSMA PET/CT identified 579 lesions (83%). In 69 identical bone lesions fluoride PET/CT showed significantly higher uptake (mean SUV_{max}:73.1 ± 36.8) compared to PSMA PET/CT (34.5 ± 31.4; $p < 0.001$). PSA at scan was correlated with SUV_{max} of PSMA PET/CT ($r = 0.58$; $p = 0.01$). No correlation was observed between PSA and fluoride PET/CT measurements. Compared to CE-CT, PSMA PET/CT showed better diagnostic performance in locating local (96% vs 61%, $p = 0.004$) and lymph node (94% vs 46%, $p < 0.001$) metastasis.

Conclusion: PSMA PET/CT was able to detect majority of bone lesions that were positive on fluoride PET/CT and was better correlated with PSA at time of scan. Further, this study indicates better diagnostic performance of PSMA PET/CT to locate soft tissue lesions compared to CE-CT.

Background

In prostate cancer (PCa) patients, spread to the skeletal system is common with progressive disease and approximately 80% of patients show bone metastasis in advanced stage [1, 2]. Bone provides an environment rich in factors that facilitate survival and stimulate growth of metastatic tumour cells. Interaction of tumour cells with local bone matrix leads to an osseous response dominated by excess osteoblastic activity [3–6], resulting in formation of predominantly osteoblastic bone lesions most commonly located in axial skeleton.

The presence of bone metastasis has a profound impact on patient prognosis with a shorter cancer specific mortality free survival of 24 months [7]. Thus, accurate early detection of bone spread throughout PCa disease progression is important to reduce potential complications and to provide optimal treatment. This challenge is further amplified by the continuous development of new imaging techniques. Through a range of imaging techniques currently available to detect bone lesions, the choice of selection for the

clinicians is more complex. Further, the chosen imaging modality must be able to accurately visualize the site of bone metastasis.

Bone scintigraphy (BS) with [^{99m}Tc]Tc-methylene diphosphonate (MDP) is used in the diagnostic work-up of PCa patients with bone lesions. BS is a relatively inexpensive technique with the advantage of broad availability and a large body of validation. On BS, MDP is incorporated into the hydroxyapatite matrix of bone in proportion to osteoblastic activity and allows the visualization of bone lesions. The tumour volume on a BS can be quantified with bone scan index (BSI) [8, 9], an independent prognostic biomarker of survival [10–13]. Currently, conventional BS is still considered the international standard and recommended in the guidelines for management of PCa patients with bone metastasis [14, 15]. However, BS has several limitations such as poor anatomical correlation, low sensitivity and specificity. As per European Association of Urology (EAU) guidelines BS should not be recommended in biochemical relapse patients with PSA below 10 ng/mL due to high probability for negative findings [14, 15]. Further, BS is often complemented by diagnostic CT to rule out false positive uptake in focal degenerative bone disease, evaluate fracture risk and to diagnose soft tissue metastasis.

Prior to use of [^{99m}Tc]Tc-MDP, [^{18}F]-sodium fluoride (NaF) with a similar uptake mechanism was approved for bone imaging but the relatively short half-life and high energy of ^{18}F limited its use with gamma cameras at that time. However, the growing popularity of PET/CT with improved detection prompted the resurgence of fluoride PET/CT. Further, more rapid blood clearance, high bone-to-background ratio and shorter examination time favoured the use of fluoride PET/CT over BS. Several studies have shown superiority of fluoride PET/CT compared to BS in terms of sensitivity and specificity [16–18].

With respect to other PET tracers, accuracy of ^{18}F- or ^{11}C- choline PET/CT in detection of bone lesions was identical but with higher specificity compared to fluoride PET/CT [16, 19]. Further, choline-PET/CT showed promising results for the early detection of bone metastasis [16]. A systematic review from 2016 concluded that fluoride-based, acetate-based and choline-based PET/CT are the most sensitive and adequate imaging techniques [20]. In recent years, ^{68}Ga-PSMA-11, targeting prostate specific membrane antigen (PSMA), was successfully introduced into clinical practice [21, 22]. Results from comparative studies showed that PSMA PET/CT outperformed commonly used tracers in localizing lesions in PCa recurrent patients [23–25].

At our institution fluoride PET/CT is commonly recommended over BS to identify bone metastasis in PCa patients at primary staging of high-risk cancer at biochemical relapse. Recently, PSMA PET/CT is introduced at our hospital and it is planned to switch to PSMA PET/CT as a clinical routine for re-staging of PCa. In the scope of PSMA PET/CT for clinical routine, both scans need to be compared and validated. Therefore, the primary aim of this study was to compare and evaluate diagnostic performance of fluoride PET/CT and PSMA PET/CT in identifying bone metastasis in PCa relapse patients. Further, comparison of PSMA PET/CT and CE-CT to detect soft tissue lesions was set as a secondary objective.

Methods

Patient characteristics

Twenty-eight patients were internally referred for PET imaging with high suspicion of widespread disease. Three patients had curative first-line therapy, five patients were given second-line treatment following first-line therapy and in 20 patients additional third-line therapy was offered prior to PET scan. In this prospective study both PSMA and fluoride PET/CT scans were acquired within one week in 27 subjects and in one subject the time interval was 15 days. All relevant clinical data including PSA at time of scan, PSA doubling time (PSA_{DT}), PSA velocity (PSA_{Vel}), Gleason score (GS) and age were recorded. The study was approved by the regional ethics review board (Dnr. 2017/190). Written informed consent was obtained from all research subjects.

Production of ^{68}Ga-PSMA-11 and ^{18}F-NaF

^{68}Ga-PSMA-11 (^{68}Ga-PSMA-11: ^{68}Ga-Glu-NH-CO-NH-Lys(Ahx)-HBED-CC (ABX, Germany) was synthesized on a fully automated synthesis platform (Modular-lab, PharmTracer; Eckert & Ziegler, Eurotope, Berlin, Germany) using dedicated disposable cassettes (C4-Ga68-PSMA, Eckert & Ziegler, Germany) [26] in accordance to good manufacturing practice (GMP) guidelines. Pharmaceutical grade ^{68}Ge/^{68}Ga generator (GalliaPharm, 50 mCi, Eckert&Ziegler, Germany) was used to produce gallium-68. The product was formulated in saline containing less than 10% of ethanol and sterile filtered (0.22 μm).

^{18}F-NaF was produced on in-house built automated system on a cyclotron (17 MeV, Scanditronix) from $H_2{}^{18}O$, and was trapped on the QMA-cartridge that then was washed with sterile water. The product was eluted with sterile physiological phosphate buffer saline and passed through a sterile 0.22 μm filter.

PET/CT imaging protocol

All PET/CT examinations were performed on a Discovery MI PET/CT system (GE Healthcare, Waukesha, WI) with a spatial resolution of 4 mm at the centre of the field of view and 2 min acquisition per bed position. After obtaining a CT transmission scan (140 kV, 40–80 mA) without contrast medium, emission scans from mid-thigh to skull base were acquired. PET scans were acquired 63 ± 5 min (range 59–75 min) after intravenous administration of 1.6 ± 0.5 MBq/kg (range 0.8–2.7 MBq/kg) of PSMA and 64 ± 12 min (range 47–97 min) after intravenous administration of 3.1 ± 0.3 MBq/kg (range 2.4–3.8 MBq/kg) of fluoride. A CE-CT scan was performed immediately after fluoride PET.

PSMA PET images were reconstructed using a block-sequential regularized expectation maximization (BSREM) (Q.Clear; GE Healthcare) method with β-value 900 [27]. Ordered subsets expectation maximization (OSEM) (VPFX-S; GE Healthcare) method with 3 iterations, 16 subsets, and a 5-mm gaussian post processing filter was used for Fluoride PET image reconstruction.

Image analysis

Hermes Hybrid Viewer version 2.0.0 (Hermes Medical Solutions AB, Stockholm, Sweden) was used for PET/CT image analysis. All bone lesions with focal uptake above the background activity of normal bone and high suspicion for malignancy were identified on both PSMA and fluoride PET/CT scans. Along with bone metastases, soft tissue lesions were also counted on PSMA PET/CT. Two observers (V.I., N.R.) independently reviewed CE-CT findings for identification of metastatic bone lesions, one of the observers (V.I.) was completely blinded to PET information.

Tracer uptake in positive lesions was measured as standardized uptake values (SUV). SUV was defined as a ratio of radioactivity concentration in region of interest (Bq/mL) and injected dose (Bq) divided by body weight (g). Maximum and mean SUV (SUV_{max}, SUV_{mean}) and tumour volume (TV) were calculated by placing a volume of interest (VOI) over pathological lesions having a fixed isocontour threshold on both scans. Total tumour volume (TTV = sum of TV of all lesions) and total lesion activity (TLA = sum of SUV_{max}*TV of all lesions) were calculated for all positive bone lesions on fluoride and PSMA PET/CT. Due to higher reproducibility, SUV_{max} was chosen for comparison. In patients having multiple bone lesions, ten bone lesions with highest SUV_{max} were separated from which identical bone lesions on both PET scans were considered for direct comparison of SUV_{max} among the two scans.

Statistical analysis

Data were presented as mean ± SD. Wilcoxon signed-rank test was used for comparison of SUV_{max} of bone lesions. Student t-test were used to compare the difference in mean PSA at time of scan between patients with negative and positive PET scans. McNemar test was used to compare the number of lesions on PSMA and fluoride PET/CT scans. Inter reader agreement on reviewing CT findings was evaluated using kappa coefficient. PSA, PSA kinetics and SUV_{max} from both PET scans were normalized using log transformation and the correlation among them was examined using univariate analysis.

Results

Patient characteristics are summarized in Table 1. Average age of the patients was 70.4 ± 7.4 years (range 55–82, median 70) with a mean PSA level of 205.4 ± 688.2 ng/mL (range 2.2–3456, median 23) at time of diagnosis. Mean PSA measured at time of the first scan was 50.8 ± 92.5 ng/mL (range 0.7–341, median 7.6).

Table 1
Patient characteristics. Gleason grade group (GG) was defined using revised International Society of Urological Pathologists (ISUP) system. Both GG and PSA at diagnosis were not retrievable in two subjects.

Patient No.	age (years)	ISUP GG	PSA at diagnosis	PSA at scan	Fluoride (MBq)	PSMA (MBq)	time diff. (days)
1	62	2	2.2	29	264	182	7
2	65	3	71	4.4	256	142	7
3	78	-	38	0.7	194	175	5
4	62	1	8.7	9.5	337	196	5
5	82	-	3456	276	231	150	2
6	80	4	200	1.9	227	163	2
7	73	1	9	341	258	144	2
8	73	5	6.9	2	307	164	7
9	78	5	26	8	239	149	7
10	75	3	7.1	42	260	123	7
11	69	4	7.2	4	256	162	7
12	76	3	7.1	5.8	256	152	7
13	64	5	112	171	268	123	7
14	65	5	9	2.3	257	186	15
15	62	5	28	32	322	183	7
16	67	5	30	20	293	114	7
17	76	5	950	7.2	333	196	7
18	79	1	18	211	292	132	7
19	65	4	69	25	263	102	7
20	80	2	9	4.3	230	91	7
21	82	2	80	177	299	138	7
22	66	3	-	6.7	295	175	7
23	69	2	-	4	309	121	7
24	61	2	128	19	280	101	7
25	55	3	5.4	4.7	422	120	7

Patient No.	age (years)	ISUP GG	PSA at diagnosis	PSA at scan	Fluoride (MBq)	PSMA (MBq)	time diff. (days)
26	74	1	20	9.4	269	115	7
27	70	3	27	2.7	246	86	5
28	64	3	16	1.9	300	83	5

No adverse reactions were observed in any of the patients after administration of fluoride and PSMA. Both scans were negative for bone metastases in 7 patients (25%). However, PSMA PET/CT detected at least one positive finding of local and/or lymph node metastases in those subjects. Mean PSA at time of scan in patients with positive bone lesions on PET scans (64.4 ± 103.5 ng/mL) was significantly elevated, compared to patients with negative bone findings (10.0 ± 14.3 ng/mL; p = 0.03).

Bone lesions were categorized into axial (spine, ribs, sternum, and skull) and appendicular (upper and lower limbs and pelvis) skeletal lesions. The pattern of detected bone lesions is shown in Fig. 1. Both scans identified bone metastases limited to axial skeleton in five patients (18%). Patients with both axial and appendicular skeletal lesions on fluoride and PSMA PET/CT scans were 16 (57%) and 15 (54%), respectively. Positive bone lesions in appendicular skeleton alone were seen with PSMA PET/CT in one subject.

In 21 of 28 included patients, 699 lesions consistent with bone lesions were detected with fluoride PET/CT. In contrast, PSMA PET/CT identified 579 bone lesions (83% of positive fluoride PET/CT lesions, $p < 0.001$) considered positive for bone metastasis. All bone lesions detected on PSMA PET/CT were also seen on fluoride PET/CT. Stratification of the patients based on number of lesions is shown in Fig. 2. Fluoride PET/CT showed less than 10 lesions in 10 patients, up to 30 lesions in three subjects and more than 30 lesions in eight patients. Whereas, PSMA PET/CT detected less than 10 lesions in 10 patients, up to 30 lesions in five subjects and more than 30 lesions in six patients. Bone metastases up to five lesions were considered as oligometastatic bone disease, fluoride PET/CT identified this in six patients whereas nine patients were detected on PSMA PET/CT. Three subjects with extensive disease burden had multiple bone lesions (> 30) in both imaging modalities. Along with bone lesions, PSMA PET/CT identified local relapse in the prostatic fossa in 7 patients and 36 positive lymph node lesions in 9 patients. Four subjects showed both positive local relapse and lymph node lesions (n = 15). A moderate but significant linear correlation was shown between PSA at time of scan and number of bone lesions on fluoride ($r = 0.48$; $p = 0.02$) and PSMA ($r = 0.46$; $p = 0.01$) PET/CT scans, respectively.

Sixty-nine identical bone lesions in 21 patients with tracer uptake on both scans were included for direct comparison. Regarding intensity of tracer accumulation, mean SUV_{max} was significantly higher on fluoride PET/CT compared to PSMA PET/CT (73.1 ± 36.8 vs 34.5 ± 31.4; $p < 0.001$). PSA_{DT} and PSA_{Vel} were available in 27 subjects with mean calculated PSA_{DT} 18.6 ± 62.4 months (range 0.8–329 months, median 4.9 months) and mean PSA_{Vel} 133.7 ± 249.7 ng/mL/year (range 0.2-1002.1 ng/mL/year, median

of 20.4 ng/mL/year). TTV from bone lesions on PSMA PET/CT strongly correlated with fluoride PET/CT TTV ($r = 0.9$, $p < 0.001$). However no correlation was seen for PSA towards TTV, TLA from both PSMA and fluoride PET/CT. Univariate analysis showed significant correlation of PSA at time of scan with highest SUV_{max} ($r = 0.58$; $p = 0.01$) and highest SUV_{mean} ($r = 0.48$; $p = 0.04$) of PSMA PET/CT. Further, PSA_{vel} also showed significant correlation with highest SUV_{max} ($r = 0.55$, $p = 0.02$) and highest SUV_{mean} ($r = 0.53$, $p = 0.02$) of PSMA PET/CT. No correlation was seen between PSA, PSA kinetics and SUV measurements from fluoride PET/CT.

Reviewing of CE-CT scans showed widespread disease (> 30 lesions) in three patients and were excluded. In the remaining 25 patients, the total number of bone lesions detected by the observers in CE-CT were 120 (V.I.) and 136 (N.R.), respectively. Substantial agreement was observed between the readers (89%, Cohen's k = 0.72) in locating bone lesions.

Findings from one blinded observer (V.I.) were considered for comparison of soft tissue lesions with PSMA PET/CT. In 12 of 28 patients, local relapse in the prostatic fossa was found, of which 11 lesions were detected with PSMA PET/CT, whereas CE-CT showed only one lesion (Fig. 3). A total of 50 lymph node lesions suspicious for cancerous lesions in 20 patients were detected using CE-CT or PSMA PET/CT (Fig. 3). Twenty-seven of 50 lymph nodes were only seen on PSMA PET/CT, whereas CE-CT alone was positive for 3 lymph nodes. Both CE-CT and PSMA PET/CT detected 20 lymph node lesions in 13 patients.

All patients had clinical follow-up and additional imaging scans at different time points were available in 21 subjects (CT in 9, Fluoride PET/CT in 4, PSMA PET/CT in 4, BS in 2, WB-MRI in one and ultrasound in one subjects). Additional scans were not performed in seven patients. Among the four subjects with PSMA-PET/CT at follow-up several bone lesions with initially positive fluoride/negative PSMA findings were PSMA -positive at follow-up. Several instances of positive PSMA/negative fluoride PET/CT were seen in subjects with wide-spread bone disease, but none of these lesions could be adequately evaluated by follow-up imaging.

Discussion

This was a prospective study in PCa patients with suspected bone metastases to evaluate the performance of PSMA PET/CT compared to fluoride PET/CT. The results suggested that PSMA PET/CT was able to detect most of the bone lesions (83%) that were positive on fluoride PET/CT. Furthermore, moderate but significant correlation of PSA at time of scan with number of bone metastases and SUV_{max} supports the use of PSMA PET/CT as the most optimal imaging tool for restaging of PCa.

The usefulness of PSMA PET/CT has primarily been investigated with a focus on localizing biochemical relapse of PCa [21, 25, 28]. A number of studies (summarized in supplementary table 1) have investigated the diagnostic accuracy of PSMA PET/CT regarding bone metastasis compared to BS [29, 30]. In addition, few studies compared the diagnostic performance of several clinically available imaging

modalities in localizing bone spread in PCa patients [31–37]. These studies showed better diagnostic performance of fluoride PET/CT and PSMA PET/CT compared to other modalities such as BS, SPECT/CT, WB-MRI, and choline PET/CT [see supplementary Table 1 for details]. Further, PSMA PET/CT showed additional value with improved specificity but with an overlapping sensitivity in comparison to fluoride PET/CT. The results from this study on comparison of PSMA PET/CT with fluoride PET/CT were also in line with these studies.

One important finding from this study is a higher detection rate of fluoride PET/CT compared to -PSMA PET/CT (699 vs 579 bone lesions). In comparison to our study, a retrospective study with a smaller data set (n = 16) conducted by Uprimny et al. also documented higher detection rate of fluoride PET/CT [38]. In that study, the authors observed low uptake of PSMA in osteosclerotic lesions similar to [28], stated as the possible explanation for low detection rate of bone lesions on PSMA PET/CT. In concordance, we also noticed overall low intensity of PSMA uptake in sclerotic bone lesions (Fig. 4). However, PSMA-PET had the influential role with its ability to detect non-osseous PCa spread. In seven patients without bone disease on both PET scans, the presence of lymph node lesions on PSMA-PET/CT changed the treatment decision.

Determining the presence of oligo-metastatic bone lesions, the potential targets for metastatic-directed therapies are clinically relevant as they can be irradiated. In the six patients who were identified with oligo-metastatic bone lesions with both PSMA and fluoride PET/CT, one patient showed additional non-osseous lesions on PSMA PET/CT, altering the treatment plan. The remaining five subjects received radiation therapy. Three more patients were identified with oligo-metastatic bone status on PSMA PET/CT but having more than five lesions on fluoride PET/CT. In addition to bone lesions, PSMA PET/CT also showed either local relapse or lymph node lesions in these patients which influenced the treatment management. However, this cohort is not large enough to determine the added value of PSMA PET/CT treatment decisions related to oligometastatic disease.

Several prospective studies showed that the detection rate of PSMA PET/CT depends on PSA levels but, due to occasionally very high receptor expression, small lesions can sometimes be visualised even at PSA levels as low as 0.2 ng/mL [36, 39]. Concordantly, our study with focus on skeletal metastasis also showed that number of bone lesions on PSMA PET/CT is associated with PSA levels at time of scan ($r = 0.45$, $p = 0.02$). Furthermore, significant difference in PSA levels between patients with positive and negative bone findings (64.4 ng/mL vs 10.0 ng/mL, $p = 0.03$) supports the association of PSMA PET/CT positivity rate and PSA. Despite the strong correlation of tumour volume and disease burden between PSMA and fluoride PET/CT, none of these metrics correlated with PSA. PSA did not predict tumour burden in the given cohort. However, strong correlation of tumour burden with fluoride PET/CT favours the use of PSMA PET/CT.

The choice of imaging techniques for restaging of PCa at a given centre depends on local parameters such as cost-effectiveness, accessibility and expertise. Many hospitals in Sweden still use BS along with an abdominal CE-CT scan as standard in the diagnostic workup. Fluoride PET/CT is generally considered

superior to ^{99m}Tc-MDP-BS and ^{99m}Tc-MDP-SPECT/CT for detection of bone metastasis [35, 40, 41]. In further support, few studies evaluated the impact of fluoride PET/CT on patient prognosis [42, 43]. At our hospital, fluoride PET/CT is recommended over BS in PCa re-staging to locate early signs of bone disease and is generally performed with CE-CT to detect soft tissue lesions.

Using follow-up scanning we could show that some lesions are detected earlier with fluoride PET/CT than with PSMA PET/CT. In none of these cases did the higher sensitivity of fluoride PET/CT lead to therapy changes and the measured tumour burden was similar for both tracers. However, equivocal skeletal findings on fluoride PET/CT are relatively common and contribute to false positive cases [32, 35], which might require additional diagnostic procedures. In this study, we also found equivocal bones lesions on PSMA PET/CT, but the overall perception is that this is a smaller problem with PSMA than with fluoride PET/CT. In addition, PSMA PET/CT provided additional information in detecting local recurrences and lymph node metastases, thus influencing the management, as seen in 7 subjects in our current study. Further, PSMA-PET can be used to select patients with potential benefit from targeted radioligand therapies using ^{177}Lu [44] and ^{225}Ac.

This study has several limitations. It was based on a small selective group of patients with high suspicion for widespread disease involving bone. A standard reference, preferably histological reports, to confirm the positive findings of PET imaging is missing. However, accessing bone for biopsy collection is neither ethically nor practically possible in all lesions. Follow-up scans with optimal imaging modalities were not available in all patients.

Conclusions

In this prospective comparative study PSMA PET/CT was able to detect the majority of skeletal metastases that were positive on fluoride PET/CT and was better correlated with PSA at time of scan. Further, better diagnostic performance of PSMA PET/CT to locate soft tissue lesions compared to CE-CT favours the use of PSMA PET/CT as the more relevant molecular imaging method for re-staging of PCa recurrence.

Declarations

Ethical approval and consent to participate

All procedures performed in studies involving human participants were in accordance with the ethical standards of the institutional and national research committee with the principles of the 1964 Declaration of Helsinki and its later amendments. Ethical approval for this prospective study was obtained from the Regional ethical review board (Dnr. 2017/190). Informed consent was obtained from all individual participants included in the study.

Consent for publication

Not applicable

Availability of data and material

The datasets used and/or analysed during this study are available from the corresponding author on reasonable request.

Competing interests

The authors declare that they have no competing interests.

Funding

Swedish cancer society (CAN2016/835) funded this study.

Authors' contributions

N.R., S.J., V.K., and J.S. conceptualized and designed the study. S.J and V.K. recruited the subjects. N.R. drafted the text and performed statistical analysis. N.R., C.T., V.I. and J.S. performed PET image analysis. M.L. and E.L. designed and validated PET reconstructions. J.S. supervised and financed the project. I.V. and J.S contributed feedback during the entire writing process. All authors reviewed and approved the final manuscript.

Acknowledgments

This work was supported by Swedish Cancer Society (CAN2016/835). The authors wish to express a sincere thanks to the Uppsala PET Centre staff for their dedicated efforts.

References

1. Herrera FGTT, Berthold DR. Bone cancer: Primary bone cancers and metastases. 2nd ed. San Diego: Elsevier; 2015.
2. Hernandez RK, Wade SW, Reich A, Pirolli M, Liede A, Lyman GH. Incidence of bone metastases in patients with solid tumors: analysis of oncology electronic medical records in the United States. BMC Cancer. 2018;18(1):44.

3. Fornetti J, Welm AL, Stewart SA. Understanding the Bone in Cancer Metastasis. J Bone Miner Res. 2018;33(12):2099–113.
4. Buenrostro D, Mulcrone PL, Owens P, Sterling JA. The Bone Microenvironment: a Fertile Soil for Tumor Growth. Curr Osteoporos Rep. 2016;14(4):151–8.
5. Wang M, Xia F, Wei Y, Wei X. Molecular mechanisms and clinical management of cancer bone metastasis. Bone Res. 2020;8:30.
6. Quiroz-Munoz M, Izadmehr S, Arumugam D, Wong B, Kirschenbaum A, Levine AC. Mechanisms of Osteoblastic Bone Metastasis in Prostate Cancer: Role of Prostatic Acid Phosphatase. J Endocr Soc. 2019;3(3):655–64.
7. Gandaglia G, Karakiewicz PI, Briganti A, Passoni NM, Schiffmann J, Trudeau V, et al. Impact of the Site of Metastases on Survival in Patients with Metastatic Prostate Cancer. Eur Urol. 2015;68(2):325–34.
8. Ulmert D, Kaboteh R, Fox JJ, Savage C, Evans MJ, Lilja H, et al. A Novel Automated Platform for Quantifying the Extent of Skeletal Tumour Involvement in Prostate Cancer Patients Using the Bone Scan Index. Eur Urol. 2012;62(1):78–84.
9. Nakajima K, Edenbrandt L, Mizokami A. Bone scan index: A new biomarker of bone metastasis in patients with prostate cancer. Int J Urol. 2017;24(9):668–73.
10. Ali A, Hoyle AP, Parker CC, Brawley CD, Cook A, Amos C, et al. The Automated Bone Scan Index as a Predictor of Response to Prostate Radiotherapy in Men with Newly Diagnosed Metastatic Prostate Cancer: An Exploratory Analysis of STAMPEDE's "M1|RT Comparison". Eur Urol Oncol. 2020;3(4):412–9.
11. Wiyanto J, Shintawati R, Darmawan B, Hidayat B, Kartamihardja AHS. Automated Bone Scan Index as Predictors of Survival in Prostate Cancer. World J Nucl Med. 2017;16(4):266–70.
12. Armstrong AJ, Anand A, Edenbrandt L, Bondesson E, Bjartell A, Widmark A, et al. Phase 3 Assessment of the Automated Bone Scan Index as a Prognostic Imaging Biomarker of Overall Survival in Men With Metastatic Castration-Resistant Prostate Cancer: A Secondary Analysis of a Randomized Clinical Trial. JAMA Oncol. 2018;4(7):944–51.
13. Miyoshi Y, Uemura K, Kawahara T, Yoneyama S, Hattori Y, Teranishi J-i, et al. Prognostic Value of Automated Bone Scan Index in Men With Metastatic Castration-resistant Prostate Cancer Treated With Enzalutamide or Abiraterone Acetate. Clin Genitourin Cancer. 2017;15(4):472–8.
14. Cornford P, Bellmunt J, Bolla M, Briers E, De Santis M, Gross T, et al. EAU-ESTRO-SIOG Guidelines on Prostate Cancer. Part II: Treatment of Relapsing, Metastatic, and Castration-Resistant Prostate Cancer. Eur Urol. 2017;71(4):630–42.
15. Mottet N, Bellmunt J, Bolla M, Briers E, Cumberbatch MG, De Santis M, et al. EAU-ESTRO-SIOG Guidelines on Prostate Cancer. Part 1: Screening, Diagnosis, and Local Treatment with Curative Intent. Eur Urol. 2017;71(4):618–29.
16. Beheshti M, Rezaee A, Geinitz H, Loidl W, Pirich C, Langsteger W. Evaluation of Prostate Cancer Bone Metastases with 18F-NaF and 18F-Fluorocholine PET/CT. J Nucl Med. 2016;57(Supplement 3):55S–

60S.

17. Langsteger W, Rezaee A, Pirich C, Beheshti M. 18F-NaF-PET/CT and 99mTc-MDP Bone Scintigraphy in the Detection of Bone Metastases in Prostate Cancer. Semin Nucl Med. 2016;46(6):491–501.
18. Cook GJR, Azad G, Padhani AR. Bone imaging in prostate cancer: the evolving roles of nuclear medicine and radiology. Clin Transl Imaging. 2016;4(6):439–47.
19. Wondergem M, van der Zant FM, van der Ploeg T, Knol RJJ. A literature review of 18F-fluoride PET/CT and 18F-choline or 11C-choline PET/CT for detection of bone metastases in patients with prostate cancer. Nucl Med Commun. 2013;34(10):935–45.
20. Wibmer AG, Burger IA, Sala E, Hricak H, Weber WA, Vargas HA. Molecular Imaging of Prostate Cancer Radiographics. 2016;36(1):142–59.
21. Afshar-Oromieh A, Avtzi E, Giesel FL, Holland-Letz T, Linhart HG, Eder M, et al. The diagnostic value of PET/CT imaging with the 68Ga-labelled PSMA ligand HBED-CC in the diagnosis of recurrent prostate cancer. Eur J Nucl Med Mol Imaging. 2015;42(2):197–209.
22. Afshar-Oromieh A, Malcher A, Eder M, Eisenhut M, Linhart HG, Hadaschik BA, et al. PET imaging with a [68Ga]gallium-labelled PSMA ligand for the diagnosis of prostate cancer: biodistribution in humans and first evaluation of tumour lesions. Eu J Nucl Med Mol Imaging. 2013;40(4):486–95.
23. Diao Wei JZ, Liao Xinyang. Recent Advances in Prostate-Specific Membrane Antigen-Based Radiopharmaceuticals. Curr Top Med Chem. 2019;19(1):33–56.
24. Calais J, Ceci F, Eiber M, Hope TA, Hofman MS, Rischpler C, et al. 18F-fluciclovine PET-CT and 68Ga-PSMA-11 PET-CT in patients with early biochemical recurrence after prostatectomy: a prospective, single-centre, single-arm, comparative imaging trial. Lancet Oncol. 2019;20(9):1286–94.
25. Afshar-Oromieh A, Zechmann CM, Malcher A, Eder M, Eisenhut M, Linhart HG, et al. Comparison of PET imaging with a (68)Ga-labelled PSMA ligand and (18)F-choline-based PET/CT for the diagnosis of recurrent prostate cancer. Eur J Nucl Med Mol Imaging. 2014;41(1):11–20.
26. Eder M, Schafer M, Bauder-Wust U, Hull WE, Wangler C, Mier W, et al. (68)Ga-complex lipophilicity and the targeting property of a urea-based PSMA inhibitor for PET imaging. Bioconjug Chem. 2012;23.
27. Lindström E, Velikyan I, Regula N, Alhuseinalkhudhur A, Sundin A, Sörensen J, et al. Regularized reconstruction of digital time-of-flight (68)Ga-PSMA-11 PET/CT for the detection of recurrent disease in prostate cancer patients. Theranostics. 2019;9(12):3476–84.
28. Eiber M, Maurer T, Souvatzoglou M, Beer AJ, Ruffani A, Haller B, et al. Evaluation of Hybrid 68Ga-PSMA Ligand PET/CT in 248 Patients with Biochemical Recurrence After Radical Prostatectomy. J Nucl Med. 2015;56(5):668–74.
29. Pyka T, Okamoto S, Dahlbender M, Tauber R, Retz M, Heck M, et al. Comparison of bone scintigraphy and 68Ga-PSMA PET for skeletal staging in prostate cancer. Eur J Nucl Med Mol Imaging. 2016;43(12):2114–21.
30. Janssen J-C, Meißner S, Woythal N, Prasad V, Brenner W, Diederichs G, et al. Comparison of hybrid 68Ga-PSMA-PET/CT and 99mTc-DPD-SPECT/CT for the detection of bone metastases in prostate

cancer patients: Additional value of morphologic information from low dose CT. Eur Radiol. 2018;28(2):610–9.

31. Dyrberg E, Hendel HW, Huynh THV, Klausen TW, Løgager VB, Madsen C, et al. 68Ga-PSMA-PET/CT in comparison with 18F-fluoride-PET/CT and whole-body MRI for the detection of bone metastases in patients with prostate cancer: a prospective diagnostic accuracy study. Eur Radiol. 2019;29(3):1221–30.
32. Fonager RF, Zacho HD, Langkilde NC, Fledelius J, Ejlersen JA, Haarmark C, et al. Diagnostic test accuracy study of (18)F-sodium fluoride PET/CT, (99m)Tc-labelled diphosphonate SPECT/CT, and planar bone scintigraphy for diagnosis of bone metastases in newly diagnosed, high-risk prostate cancer. Am J Nucl Med Mol Imaging. 2017;7(5):218–27.
33. Jambor I, Kuisma A, Ramadan S, Huovinen R, Sandell M, Kajander S, et al. Prospective evaluation of planar bone scintigraphy, SPECT, SPECT/CT, 18F-NaF PET/CT and whole body 1.5T MRI, including DWI, for the detection of bone metastases in high risk breast and prostate cancer patients: SKELETA clinical trial. Acta Oncol. 2016;55(1):59–67.
34. Lengana T, Lawal IO, Boshomane TG, Popoola GO, Mokoala KMG, Moshokoa E, et al. 68Ga-PSMA PET/CT Replacing Bone Scan in the Initial Staging of Skeletal Metastasis in Prostate Cancer: A Fait Accompli? Clin Genitourin Cancer. 2018;16(5):392–401.
35. Poulsen MH, Petersen H, Høilund-Carlsen PF, Jakobsen JS, Gerke O, Karstoft J, et al. Spine metastases in prostate cancer: comparison of technetium-99m-MDP whole-body bone scintigraphy, [18F]choline positron emission tomography(PET)/computed tomography (CT) and [18F]NaF PET/CT. BJU Int. 2014;114(6):818–23.
36. Zacho HD, Nielsen JB, Dettmann K, Haberkorn U, Langkilde NC, Jensen JB, et al. 68Ga-PSMA PET/CT in Patients With Biochemical Recurrence of Prostate Cancer: A Prospective, 2-Center Study. Clin Nucl Med. 2018;43(8):579–85.
37. Zacho HD, Ravn S, Afshar-Oromieh A, Fledelius J, Ejlersen JA, Petersen LJ. Added value of (68)Ga-PSMA PET/CT for the detection of bone metastases in patients with newly diagnosed prostate cancer and a previous (99m)Tc bone scintigraphy. EJNMMI Res. 2020;10(1):31.
38. Uprimny C, Svirydenka A, Fritz J, Kroiss AS, Nilica B, Decristoforo C, et al. Comparison of [68Ga]Ga-PSMA-11 PET/CT with [18F]NaF PET/CT in the evaluation of bone metastases in metastatic prostate cancer patients prior to radionuclide therapy. Eur J Nucl Med Mol Imaging. 2018;45(11):1873–83.
39. Hoffmann MA, Buchholz H-G, Wieler HJ, Höfner T, Müller-Hübenthal J, Trampert L, et al. The positivity rate of 68Gallium-PSMA-11 ligand PET/CT depends on the serum PSA-value in patients with biochemical recurrence of prostate cancer. Oncotarget. 2019;10(58):6124–37.
40. Bortot DC, Amorim BJ, Oki GC, Gapski SB, Santos AO, Lima MCL, et al. 18F-Fluoride PET/CT is highly effective for excluding bone metastases even in patients with equivocal bone scintigraphy. Eur J Nucl Med Mol Imaging. 2012;39(11):1730–6.

41. Iagaru A, Mittra E, Dick DW, Gambhir SS. Prospective Evaluation of 99mTc MDP Scintigraphy, 18F NaF PET/CT, and 18F FDG PET/CT for Detection of Skeletal Metastases. Mol Imaging Biol. 2012;14(2):252–9.
42. Hillner BE, Hanna L, Makineni R, Duan F, Shields AF, Subramaniam RM, et al. Intended Versus Inferred Treatment After (18)F-Fluoride PET Performed for Evaluation of Osseous Metastatic Disease in the National Oncologic PET Registry. J Nucl Med. 2018;59(3):421–6.
43. Gareen IF, Hillner BE, Hanna L, Makineni R, Duan F, Shields AF, et al. Hospice Admission and Survival After (18)F-Fluoride PET Performed for Evaluation of Osseous Metastatic Disease in the National Oncologic PET Registry. J Nucl Med. 2018;59(3):427–33.
44. Baum RP, Kulkarni HR, Schuchardt C, Singh A, Wirtz M, Wiessalla S, et al. 177Lu-Labeled Prostate-Specific Membrane Antigen Radioligand Therapy of Metastatic Castration-Resistant Prostate Cancer: Safety and Efficacy. J Nucl Med. 2016;57(7):1006–13.

Figures

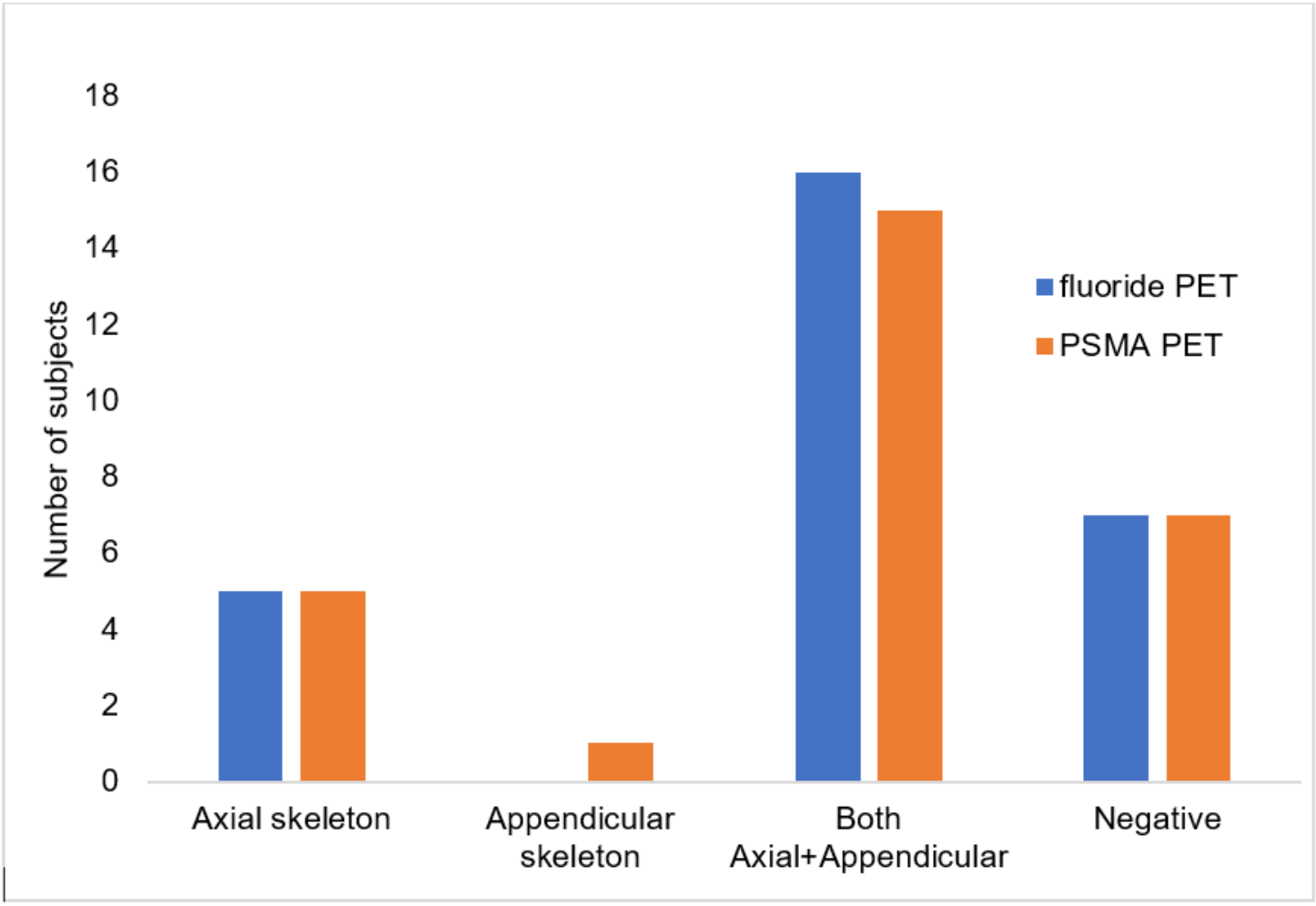

Figure 1

Pattern of detected bone lesions on both fluoride and PSMA PET. Seven patients showed negative findings and five subjects showed positive bone metastases in the axial skeleton on both scans. Bone lesions with axial and appendicular skeleton were detected in 16 patients on fluoride-PET and 15 subjects on PSMA-PET. In one patient bone lesions in appendicular skeleton were detected only on PSMA-PET.

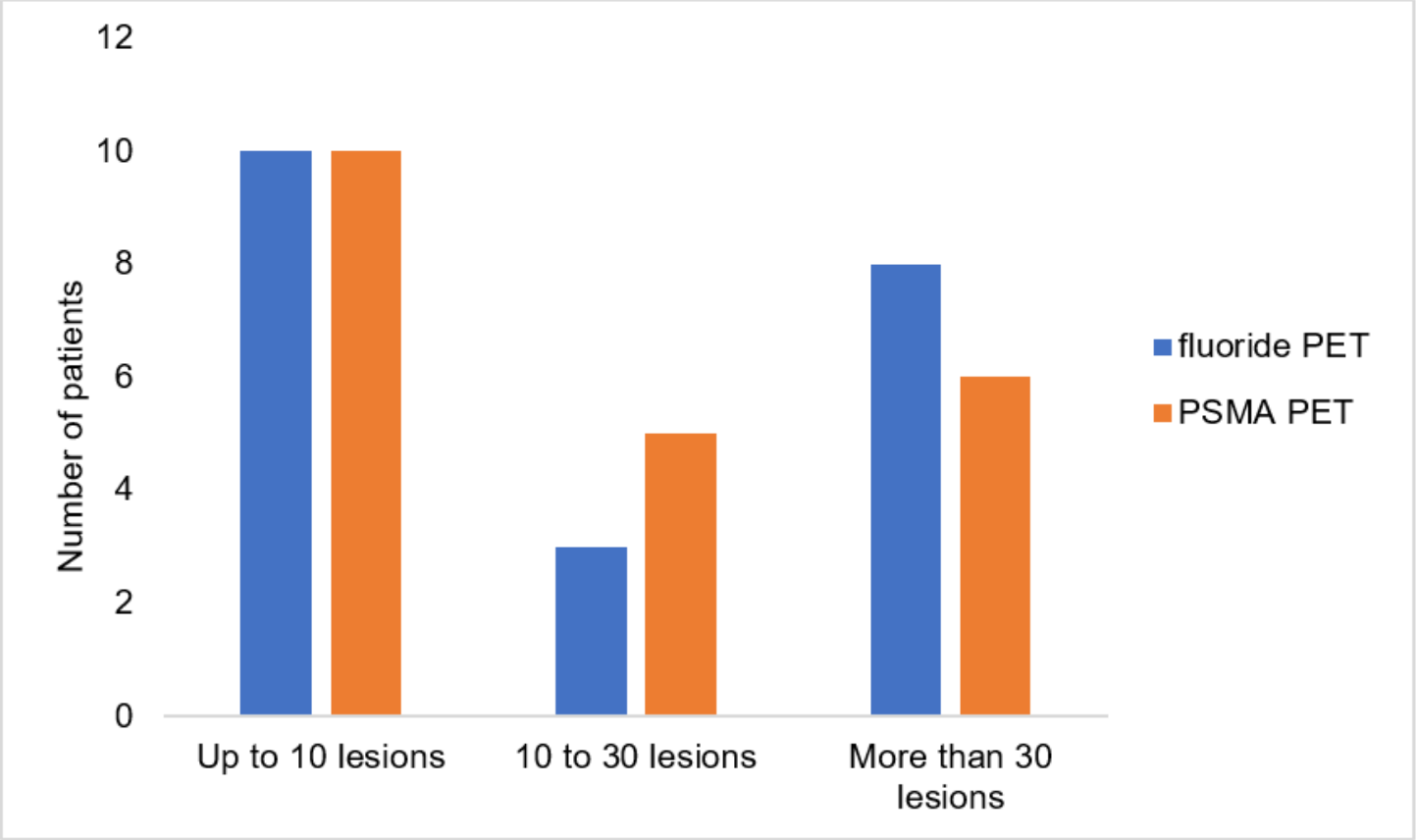

Figure 2

Patients were stratified based on number of bone lesions detected on fluoride- and PSMA- PET, excluding the negative PET scans. Both PET scans showed up to 10 bone lesions in 10 subjects. Fluoride-PET showed 10-30 bone lesions in three patients whereas PSMA identified 10-30 lesions in five subjects. Multiple bone lesions (more than 30) were detected in eight patients on fluoride-PET. PSMA-PET identified multiple bone lesions in six patients.

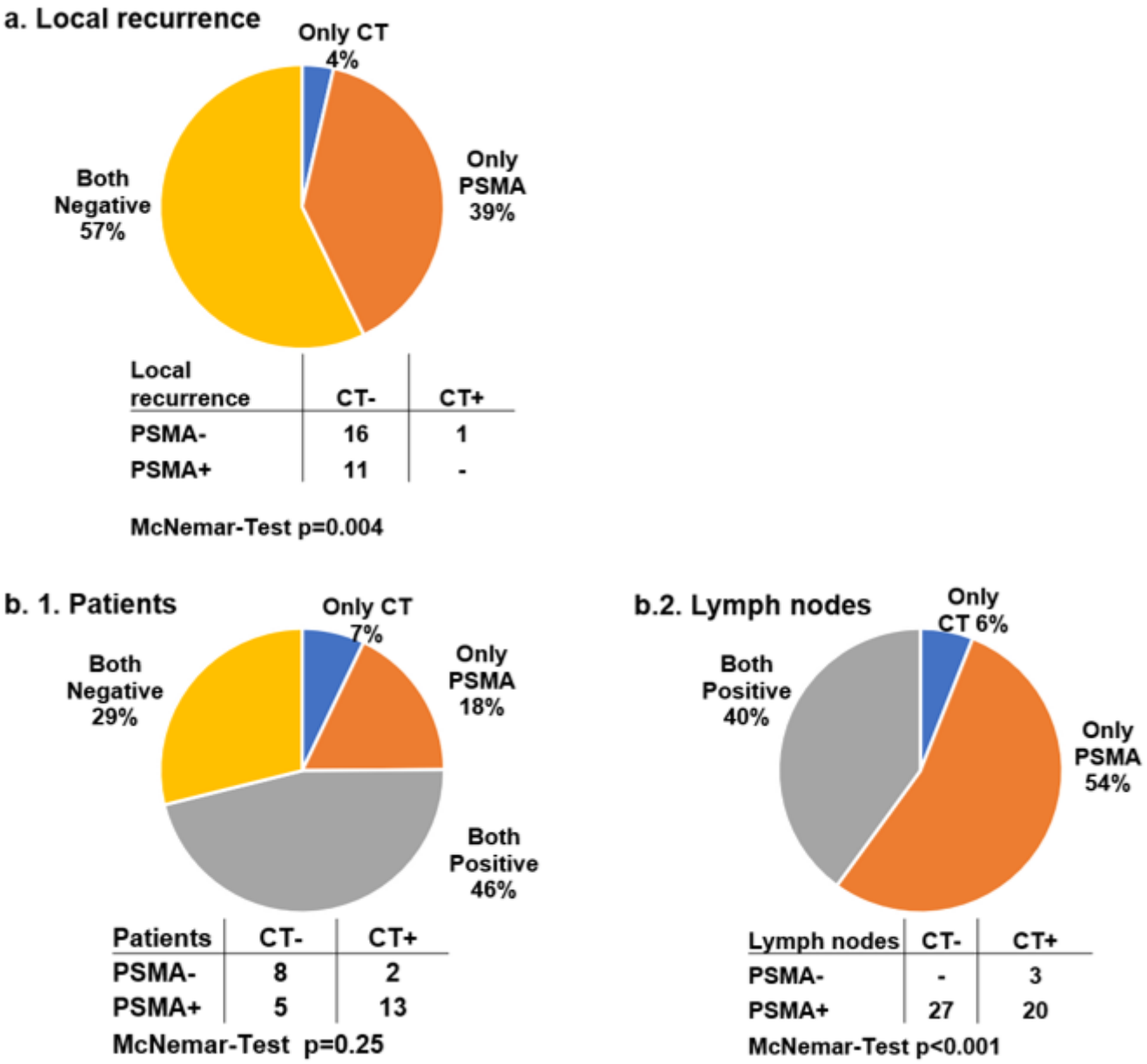

Figure 3

Suspicious local and lymph node lesions in patients with biochemical relapse. (a) Percentage and numbers of local recurrence in the prostatic fossa detected by CT and PSMA-PET. (b. 1) Percentage and number of patients with suspicious lymph nodes detected by CT and PSMA-PET. (b.2) Percentage and number of suspicious lymph nodes identified by diagnostic-CT and PSMA-PET.

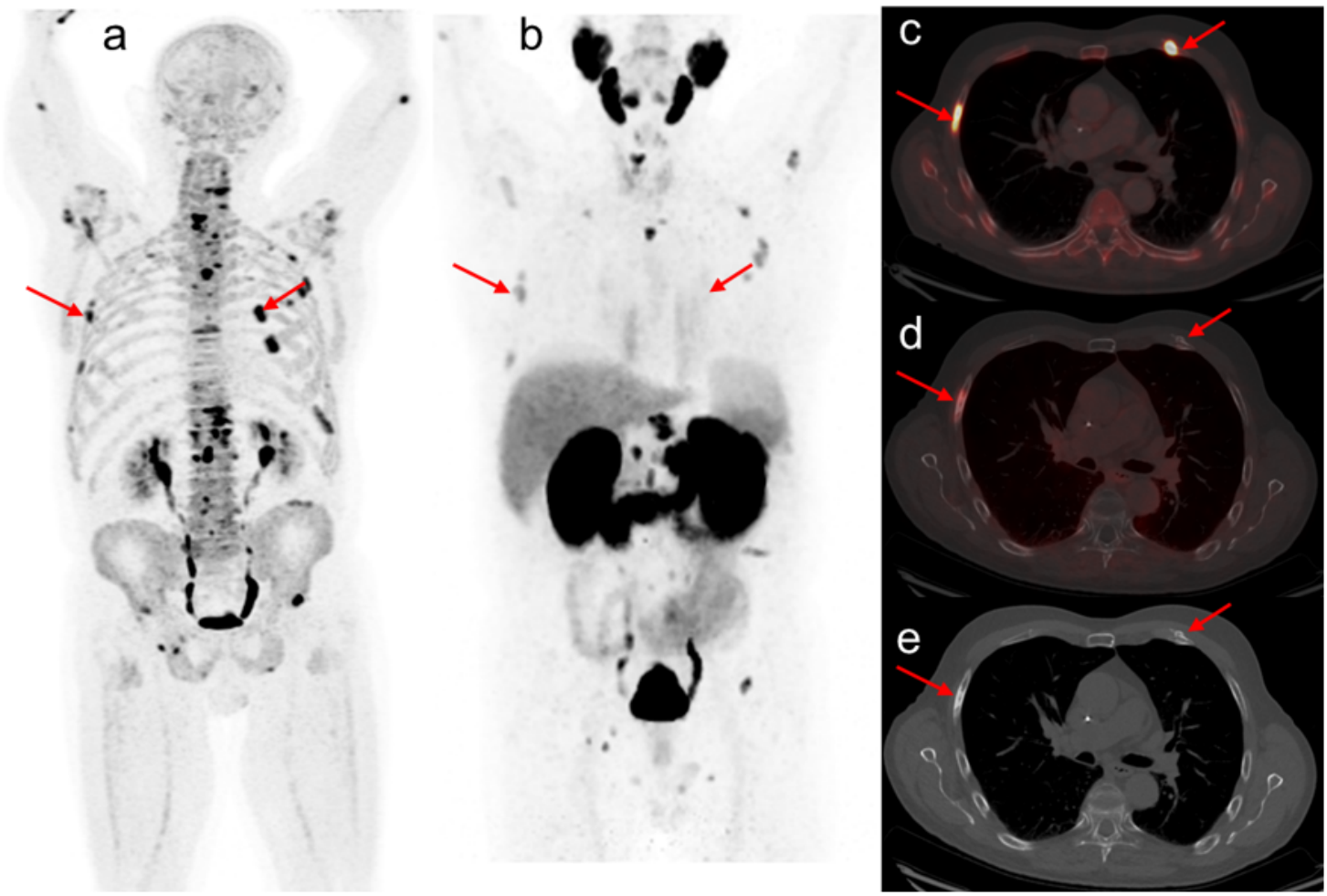

Figure 4

A 65-year-old patient diagnosed with 4+3 PCa underwent radiation, hormonal and chemotherapy and became hormone refractive. On referral, PET imaging revealed bone lesions on maximum intensity projection of fluoride-PET (a) and PSMA-PET (b). The majority of bone lesions were sclerotic in nature having high intensity uptake on fluoride-PET (a) but reduced uptake on PSMA-PET (b). Fused trans-axial PET/CT images showing two sclerotic rib lesions on fluoride-PET (C), whereas PSMA-PET showed only one sclerotic lesion (d, left arrow over rib). Respective sclerotic lesions showed on axial CT (e).

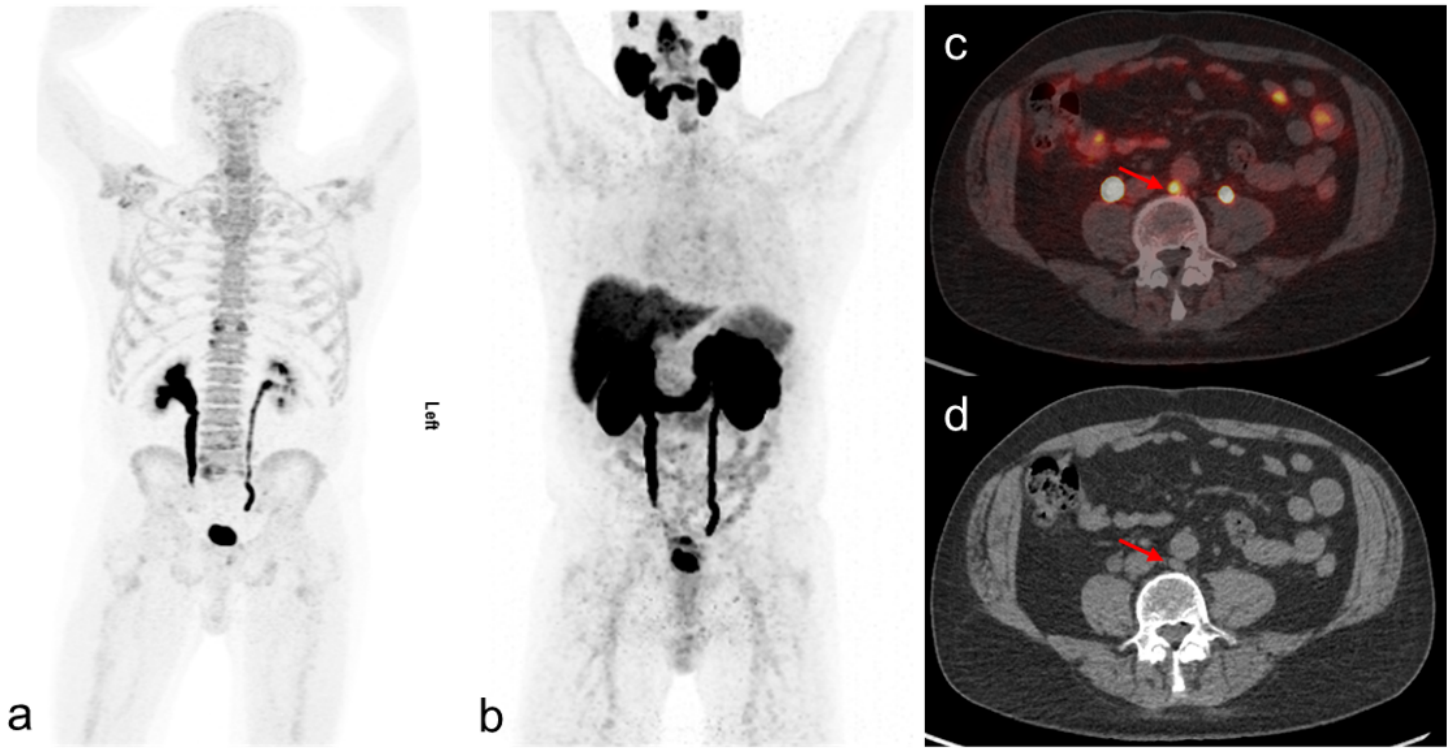

Figure 5

A 75-year-old 4+3 PCa patient treated with radiation and adjuvant hormonal therapy referred for PET imaging due to rising PSA (PSA was 42 ng/mL at time of scan). Maximum intensity projection images of both fluoride-PET (a) and PSMA-PET (b) showed negative bone lesions. However, para-aortic lymph node (red arrow) showed positive uptake on PSMA-PET (c), which also correlated with CT (d).

Supplementary Files

This is a list of supplementary files associated with this preprint. Click to download.

- Supplimentarytable.docx